

Spatial and Temporal fluctuation of an ABP in an optical trap

Chong Shen¹, Lanfang Li², Zhiyu Jiang¹, H. D. Ou-Yang^{1,2}

1. Department of Physics, Lehigh University, 16 Memorial Dr. E, Bethlehem, PA 18015, USA

2. Emulsion Polymers Institute, Lehigh University, 16 Memorial Dr. E, Bethlehem, PA 18015, USA

Abstract

Active colloidal systems contain active particle, which converts energy from the environment into directed or persistent motion. An outstanding question, debated to date, pertains to how a quantitative and well-defined means can be established to quantify the differences between the statistical behavior of an active particle and a passive Brownian particle. To address this question, we set out to investigate the motions of a single, induced-charge electrophoretic (ICEP) metallic Janus particles in a quadratic potential of an optical trap, by experiments and numerical simulations. The positions of the particle under different driving forces were measured by experiments and simulated numerically using a generalized Langevin equation. The 1-D positional histograms of the active particle, distinctively different from that of a Boltzmann distribution, reveal splitting of the positional distribution of a single peak centered at the bottom of the well into two symmetrical peaks, whose centers move away from the center to a distance increasing with the driven force. We provide a convolutional method to capture how and when the non-thermal histogram appear. The temporal fluctuations of the active particle in the well are analyzed by their power spectral density (PSD). We found that the fluctuation power spectral density (PSD) plots have two characteristic frequencies, which reveal a frequency dependent effective temperature by the fluctuation-dissipation theorem. The relationship of spatial and temporal fluctuation are discussed at the end.

Introduction

At the beginning of the 20th century, classical thermodynamics provided a comprehensive understanding of the equilibrium behavior of macroscopic systems in contact with thermal reservoirs and established a deterministic relationship between thermodynamic quantities. [1] During the past few decades, the intense research interest in the nonequilibrium systems calls for a broadened scope of thermodynamics. [2] Active matter, which is composed of the active agents, is characterized by the ability to transduce energy to the movement. [3] Active matter is important as the biological system can be categorized as an active system. Inactive matter, non-thermal fluctuations play an important role. [3] One fundamental issue is how we can use thermodynamics parameter to describe an active matter? [4,5]

As a model system, Active Brownian particle system has been used, in which the particles move at a constant speed with the direction being determined by the rotational

diffusion. [6] Previously, Boltzmann distribution was used to determine the spatial distribution of Active Brownian Particle (ABP) under a uniform force field at an effective temperature higher than ambient temperature, which is the classical equilibrium temperature. [7,8] However, the effective temperature treatment still calls for Boltzmann distribution, but recent research studies of ABP system in confinement show the collection of particles near the wall and thus the distribution is not Boltzmann any more. [9–11] The histogram of particle position (HPP) describes the particle's time-averaged probability at certain position. The simpler case of only considering the active component of the movement has been treated with mean-field theory, however, it did not encompass thermal movement component. [12] Takatori et. al. performed a set of experiments with chemical phoretic Janus particles in an acoustic trap and revealed a similar behavior to mean-field theory and simulation. [13] But Arjun et al conducted the experiments of a bacteria kicking ABP in a smaller optical trap showed deviation from the mean-field theory. [14,15] The weak trap strength of the acoustic trap study and the limited dynamic range of the bacterial bath prohibited exploration of a more complete parameter space. Until now, when and how the Boltzmann statistics would fail for ABP is still not clear. [10]

Here, a series of experiments with an optically trapped Active Brownian particle and numerical simulation are present to study the fluctuation when the system has both thermal and non-thermal noise. First, we observe a transition of histogram between a regime that can be described with Boltzmann distribution to a regime that not follows Boltzmann distribution, a double peak distribution when increasing the particle speed or decreases the spring constant. The histogram can consider as a convolution of the pure thermal histogram and a pure active histogram. Second, we show that the fluctuation power spectral density (PSD) of an active particle held in potential have two turning point, which refers to rotational diffusivity and fluctuation trap coupling. In consequence of that, the effective temperatures from fluctuation-dissipation are frequency dependent. The active PSD contribution can be separated from the passive PSD. Then, an analytical expression was obtained. Third, we also find an equivalent relationship between the integral of PSD and potential from histogram though calculating the Effective temperatures from different definitions.

Materials and Methods

We synthesized 3 μ m metallic Janus particles by depositing a thin film of metal on 3 μ m silica particles (as purchased, Bangs Laboratory, SS05N). [16] First, the 3 μ m particles (dry powder) were mixed with 300 nm polystyrene (PS) latex (40%wt) suspension at 20% volume particle 8% volume PS in water. The mixture was then deposited by vibration-assisted convective deposition method [17] to create a monolayer of 3 μ m base silica particles on a glass substrate. After drying under ambient condition, the composite microsphere monolayer on glass was then heated at 240 $^{\circ}$ C for a few minutes so the PS particles melted into a 1650 nm PS film covering the bottom half of the SiO₂ spheres. The monolayer of SiO₂ spheres, with bottom half immersed in a PS layer, was then loaded into a sputter coater (Poloran E5100) to receive a 30nm coating of Ir on the top half surface. The sample was then heated at 500 $^{\circ}$ C (Lindberg/Blue M™ Moldatherm™ Box Furnaces, BF51748C-1) for 1 hour to remove the polystyrene. The sample was then placed in a water filled centrifuge tube and sonicated in a

sonication bath (Branson, 1510) for 6 hours to release the particles, forming hemispherically coated Janus particles suspension in water. The SEM (Hitachi 4300SE) micrograph of the resultant Janus particles is shown in Fig.1 A

Janus particle can be driven by a uniform AC electric field to move in a direction perpendicular to the field. [18] We used ITO coated glass slides as transparent electrodes. The model system contained a suspension of Janus particles sandwiched between two ITO coated glass slides with 50 μ m separation, showing in Fig.1 B). A 5kHz AC voltage was applied across the electrodes to create a uniform electric field perpendicular to the electrodes. This electric field can drive the Janus particles in the horizontal direction by a mechanism of induced-charge electrophoresis (ICEP), making it a model two dimensional (2D) ABP system. [15] We tracked the particle to find the trajectory from video by ImageJ with Mosaic Suit. [19]

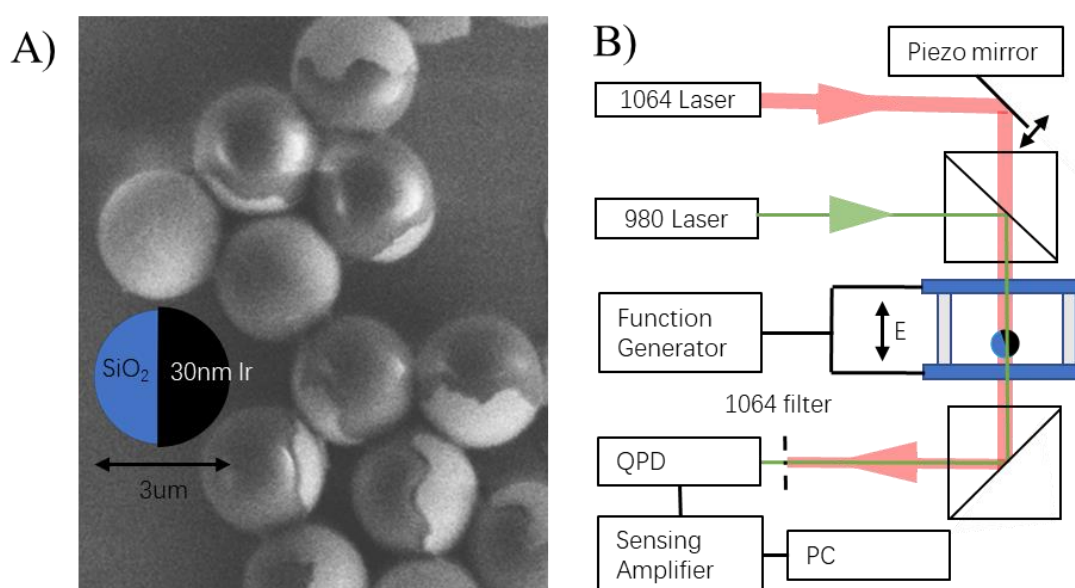


Fig.1 A) SEM image of 3.0 μ m Silica beads partially coated with iridium (Ir). Insert: sketch of the Janus particle. B) Simplified optical trap set-up with experimental chamber.

We used a 1064nm wavelength laser to create an optical trap, as shown in Fig 1.C). The stiffness of the trap was measured to be 3.0pN/ μ m with 25mw laser power by passive and active microecology. [20,21] The trap is approximately a quadratic potential well. To achieve a high temporal and spatial detection resolution of the particle position, a 980nm wavelength laser was applied to serve as a tracking beam that was aligned collinearly with the trapping laser beam. A Quadrant PhotoDiode (in-house design) was at the end of the tracking beam, analyzing the deflection of the tracking beam. As the particle information is carried by the deflection of the tracking beam, the particle position can be measured from the position of the

deflected tracking beam. Such detection scheme can achieve 5nm spatial resolution at 1 kHz sampling rate.

To avoid large scattering force on the metal cap of the particle, which has been shown to make optical trapping unstable, [22,23] we use particles with coating areas smaller than that of a hemisphere to reduce the scattering effect and make a stable trap for the particles. To ensure the effect of light scattering is negligible compared with optical trapping, we examine the Brownian motion of 3 um metallic Janus particles in an optically trap to obey the same Boltzmann distribution as that of an uncoated silica particle in the same trap. An alternative way to achieve the small-cap area is using e-beam evaporate with shadowing angle. [24]

Simulation Model

The active particle is simulated as a self-propelled particle with a constant pushing force. The direction of this force is dependent on the orientation of the particle, which randomly turns according to D_r (rotational diffusivity). Since the particle is in water in our experiments, it also has thermal Brownian motion, which randomly moves according to D_t (translational diffusivity). When the particle is in confinement, a confinement force is added into the Langevin Equation.

We can write out the Langevin Equation for the particle in 2D: [25]

$$m\ddot{r} = \hat{\theta}F_0 - \eta\dot{r} - k_{OT}r + \sqrt{2k_B T}W_{noise}$$

$$I\ddot{\theta} = -\eta'\dot{\theta} + \sqrt{2k_B T}W_{noise}$$

Where m is the mass of the particle, r is the position of the particle, θ is the orientation of particle, F_0 is the constant pushing force, η is the drag coefficient, k_{OT} is the spring constant, W_{noise} is the normalized white noise over sqrt unit time, I is the moment of inertia, η' is the rotational drag coefficient.

In water, the particle moves in the over-damping regime. So, the left part of the equations will be 0. Where we have

$$0 = \hat{\theta}F_0 - \eta\dot{r} - k_{OT}r + \sqrt{2k_B T}W_{noise}$$

$$0 = -\eta'\dot{\theta} + \sqrt{2k_B T}W_{noise}$$

Then, we can solve the Langevin Equation and write finite difference simulations:

$$\frac{dr}{dt} = \frac{\hat{\theta}F_0 - k_{OT}r + \sqrt{2k_B T}W_{noise}}{\eta}$$

$$\frac{d\theta}{dt} = \frac{\sqrt{2k_B T}W_{noise}}{\eta'}$$

With finite difference simulations of white noise, [25] replace constants with D_r and D_t . The simulation can be run step by step as the following equation:

$$\theta_{i+1} = \theta_i + \sqrt{2D_r dt}w_{noise}$$

$$x_{i+1} = x_i - \frac{\hat{\theta}F_0 dt}{\eta} - \frac{k_{OT}x dt}{\eta} + \sqrt{2D_t dt}w_{noise}$$

$$y_{i+1} = y_i - \frac{\hat{\theta}F_0 dt}{\eta} - \frac{k_{OT}y dt}{\eta} + \sqrt{2D_t dt}w_{noise}$$

Where w_{noise} is the normalized white noise.

Results and Discussion

Active Diffusion of ICEP particle

Predicted theoretically by Squires and Bazant, [26] and subsequently observed experimentally by Gangwal et al.¹², a metallic-dielectric Janus sphere will move by induced-charge electrophoresis (ICEP) away from the metal side at a velocity,

$$v(ICEP) = \frac{9}{64} \frac{\epsilon a}{\eta(1+\delta)} E^2 \quad (1)$$

where ϵ is the electric permittivity, η is the viscosity of the bulk solvent, a is the radius of the particle, E is the electric field, and δ is the ratio of the capacitances of the compact and diffuse layers.

The Mean Squared Displacement as a function of time is calculated from particle tracking data. As shown in Fig 2 A), at no applied field, the particle shows normal diffusion motion, characteristic of the slope of 1 in the MSD vs time graph. With an applied voltage, two slopes were evident: at the short-time a slope of 2 which signifies a ballistic motion; at the long-time a slope of 1 which is consistent with normal diffusion motion but with a higher diffusivity.

Translational diffusivity of particle away from the surface from Stokes-Einstein relation²⁰:

$$D_t = \frac{k_B T}{6\pi\eta r} = 0.145 \mu m^2/s \quad (2)$$

Translational diffusivity of the ABP at a long time is calculated from fitting the following equation to the experimental data in Fig. 1 A):

$$D_t = \frac{dMSD}{4dt} = 0.053 \pm 0.008 \mu m^2/s \quad (3)$$

The measured D_t is smaller than free diffusivity from Stokes-Einstein relation due to the particle is close to the bottom surface. Using Faxen's law for a single wall, the distance between the particle bottom to the surface is equal to 11.5 ± 2.1 nm. The Debye length from our system is 12.3 nm from conductivity measurement.

Rotational diffusivity calculated for particles with a radius of 1.5 microns using Einstein relation:

$$D_r = \frac{k_B T}{8\pi\eta r^3} = 0.0485/s \quad (4)$$

The transition between the mode of motion can be characterized by relaxation time [27] for ABP.

$$MSD = 4D_t t + 2v_0^2 \tau_r [t - \tau_r (1 - e^{-t/\tau_r})] \quad (5)$$

Fitting the experimental MSD data yields $\tau_r = 17.8 \pm 1.4s$, averaging from different applied electric field strengths.

We determined the proportionality constant between $v(\text{ICEP})$ and E^2 by experiment by calculate the speed from MSD, showing in Figure.1 D. The $v(\text{ICEP})$ increase linearly with E^2 and reach a plateau at around 20 $\mu\text{m/s}$. The non-Linear behavior reveals that the linear assumption of flow to the electric field may not work at high speed. Our study is in the linear region with speed of particle from 0 to 3.5 $\mu\text{m/s}$.

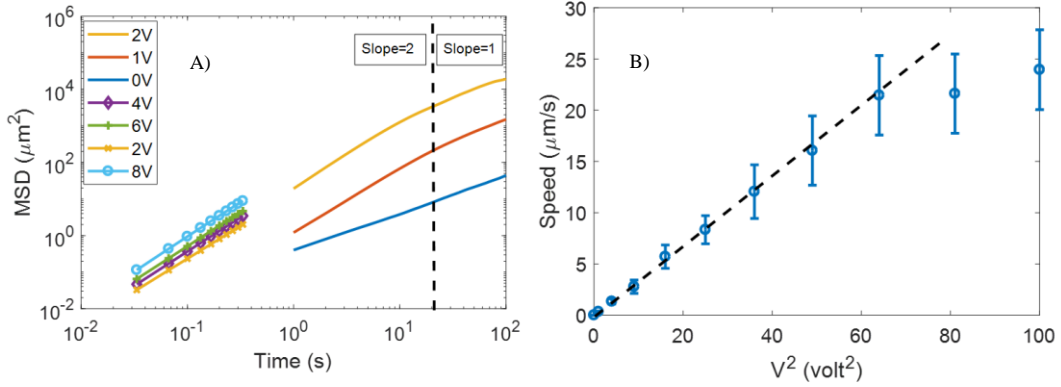


Fig. 2 A): MSD data from experiment under different voltages. C) Swim speed under different voltages. The black line refers to the linear relationship between average speed and applied voltage squared.

Spatial fluctuation (histogram) of an active particle in an optical trap

The Histogram of Particle Position (HPP) is defined here to be the normalized probability occurrence of the particle at a particular position in 1-D. [14] The HPP of an ABP is shown in the Fig.4 A. With increasing the electric field, the shape of HPP changes from Gaussian distribution to a bimodal distribution. It is well known that the thermal fluctuation follows Gaussian distribution, so it is only possible that the non-Gaussian component is from the active motion. The higher the electric field, ie., the active motion speed, the further away from the center the two peaks become.

To understand the motion of the particle, a first principle calculation was performed using the generalized Langevin equation (Eq 4) . [15,25]

$$m\ddot{r} = \hat{\theta}F_0 - \eta\dot{r} - k_{OT}r + \sqrt{2k_B T}W_{noise} \quad (6)$$

$$0 = \hat{\theta}v_0 D - \eta\dot{r} - k_{OT}r + \sqrt{2k_B T}W_{noise} \quad (7)$$

In overdamped condition, the equation becomes Eq 5, where v_0 experimentally determined from Fig 3B, the drag-coefficient being self-drag, k_{OT} experimentally determined to be 1.3 pN/ μm , W_{noise} from a random number generator matching a Gaussian profile. With no

fitting parameters, the simulation captures the essence of the motion of the particle at a first principle level. The active motion component is responsible for the separation of the Gaussian peak into bimodal distribution.

With keeping the spring constant to be 1.5pN/um and increasing the electric potential, the shape of probability changes from Gaussian distribution to a bimodal distribution. A similar transfer of probability appears in our simulation. As far as we know, we are the first time observe the bimodal distributions of an active particle in an optical trap. The bimodal distribution can be understood from the slow down of active particle when the trap force and propelling force canceled out. When slow down happens, the particle will spend more time on the slower speed rather than at the center.

While keeping the speed of particle to be a constant and decreasing the spring constant of the trap from 3pN/um to 0.8pN/um, the shape of the histogram changes from Gaussian to a flat top distribution, showing in Fig 3 B. The histogram of such a small system (size less than 1um) is more non-Gaussian in a weak trap which seems to controvert the previous theory [12] and experimental result. [13]

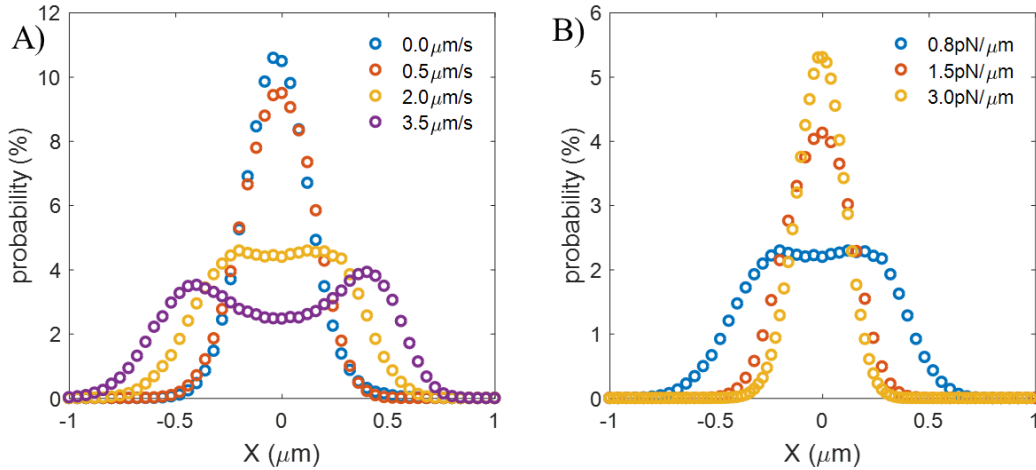


FIG. 3. a) Histogram of the particle position (HPP) of 3um Janus particles under spring constant equal to 1.5pN/um for various AC electric potential at 5 kHz. B) HPP of the position of 3um Janus particles under the optical trap with various spring constant from 0.8 pN/um to 3.0pN/um with 5V applied.

A better way to understand the histogram of ABP in a trap with thermal noise is separately considered the active noise in the trap and passive noise in the trap than use convolution to add them together. The derivation started from the Langevin equation of active particle in trap

$$m\ddot{r} = \hat{\theta}F_0 - \eta\dot{r} - k_{OT}r + \sqrt{2k_B T}W_{noise} \quad (8)$$

In over damping system (microparticle in water), the inertia can be ignored. Thus, we have

$$0 = \hat{\theta}F_0 - \eta\dot{r} - k_{OT}r + \sqrt{2k_B T}W_{noise} \quad (9)$$

Where m is the mass of the particle, r is the position of the particle, θ is the orientation of particle, F_0 is the constant pushing force, η is the drag coefficient, k_{OT} is the spring constant, W_{noise} is the normalized white noise over sqrt unit time.

Then we can consider to sperate this Langevin equation into two Langevin equations with only active motion and only thermal noise.

$$0 = \hat{\theta}F_0 - \eta\dot{r}_1 - k_{OT}r_1 \quad (10)$$

$$0 = -\eta\dot{r}_2 - k_{OT}r_2 + \sqrt{2k_B T}W_{noise} \quad (11)$$

Where $r_1 + r_2 = r$. The first equation describes a pure active motion. The second equation describes thermal motion. Let the histogram from the active motion to be $P_A(r_1)$ and the histogram from the thermal motion to be $P_P(r_2)$. The histogram r can be calculated by:

$$P(r) = P_A * P_P(r) = \int P_A(r_1)P_P(r - r_1)dr_1 \quad (12)$$

The shape of $P(r)$ is determined by the P_A or P_P with the large mean squared displacement (MSD). If P_A have the larger MSD, the shape of the $P(r)$ is dependent by $\frac{\tau k_{OT}}{\eta}$. If $\frac{\tau k_{OT}}{\eta} \gg 1$,

the $P(r)$ will be non-Gaussian, showing in Fig 4 a. If $\frac{\tau k_{OT}}{\eta} \ll 1$, the $P(r)$ will be Gaussian with

larger MSD, showing in Fig 4 b. If P_P have the larger MSD, the shape of the $P(r)$ is close to the P_A with some heavy tail, showing in Fig 4 c.

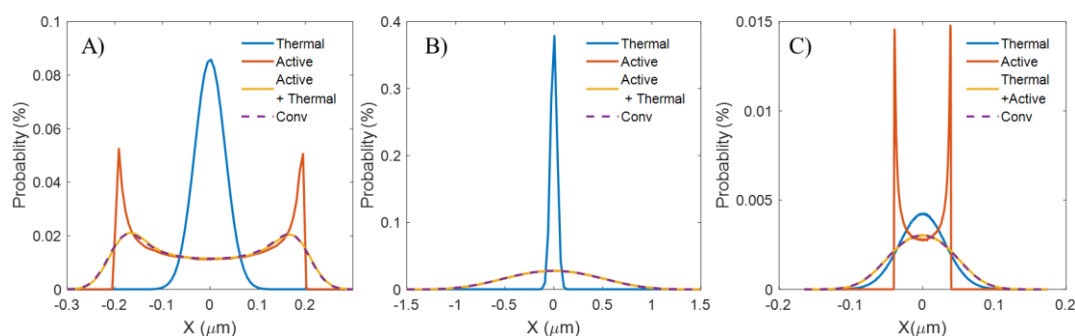


Figure 4. Simulated histogram of thermal noise (solid blue line), active noise (orange solid line), active +thermal noise (yellow solid line) and convolution (purple dash line) between the histogram of thermal noise and histogram of active noise. Different dynamic parameters are using. a) $v=10\mu\text{m/s}$ $Dr=3/\text{s}$ b) $v=100\mu\text{m/s}$ $Dr=500/\text{s}$ c) $v=2\mu\text{m/s}$ $Dr=3/\text{s}$

The convolution between histogram from thermal noise and active noise perfectly align with the histogram of active plus thermal noise. The spatial fluctuation of active particle with thermal noise that can be understood as the active fluctuation and thermal fluctuation linear add together. This find explain the opposite trend perfectly. To describe the system, a convolution method is introduced and verified in all the regime, which including our condition, larger acoustic trap [13] and even biological system. [28]

Temporal Fluctuation power spectra of an active particle in an optical trap

The fluctuation power spectral density (PSD) is the Fourier transform of the autocorrelation of the particle position, [29]

$$S_x = \frac{1}{T} \int_0^T \int_0^T \langle x(t)x(t') \rangle e^{i\omega(t-t')} dt dt' \quad (13)$$

where S_x is the power spectral density, T is the total time of integration, $\langle x(t)x(t') \rangle$ is the auto-correlation function of the particle position $x(t)$ at time t . The PSD represents the intensity of fluctuation at a certain frequency. PSD can be calculated from experimental particle tracking data.

PSD of a Brownian particle in confinement is shown as the black dash line shows in Fig.6 A. The Brownian particle PSD exhibits two linear components: a flat plateau at low frequency (0.1~10Hz) and a straight line with slope equal to -2 at high frequency (10Hz~100Hz). The characteristic frequency at which the slope changes corresponds to the competition between thermal fluctuation and optical trap confinement. For an active particle in the same trap, the PSD exhibit the same feature at higher frequencies (10~100Hz), but at lower frequencies (0.1Hz-10Hz) the PSD value increases with applied voltage. The increase at low frequency was as high as 10^5 for an active particle with 8V of applied voltage, compared to a Brownian particle. From a particle movement point of view, the high-frequency feature is determined by translational thermal diffusion and trap coupling, and the low-frequency characteristics are related to Janus particle rotational diffusion and particle active motion speed.

Fig. 5 B) shows a clear two turning point manner. These two turning points are showing in each PSD of ABP in a trap. One comes from thermal diffusion and trap coupling:

$$S(\omega) = \frac{12\pi\eta Rk}{\left(\frac{k_{OT}}{R}\right)^2 + (\eta\omega)^2} T \quad (14)$$

Another comes from rotational diffusion (labeled with red dash line)

$$S_{xxratio}(\omega) = \frac{v^2\tau^{-1}}{2D_t(\omega^2 + 4\pi^2\tau^{-2})} + 1 \quad (9)$$

The difference area on PSD reveals the energy dissipation of only active force. [28] Since, the difference of PSD only appears at low frequency, the active force doesn't a contribution to the high-frequency dissipation. The contribution frequency is controlled by its own relaxation time of reorientation.

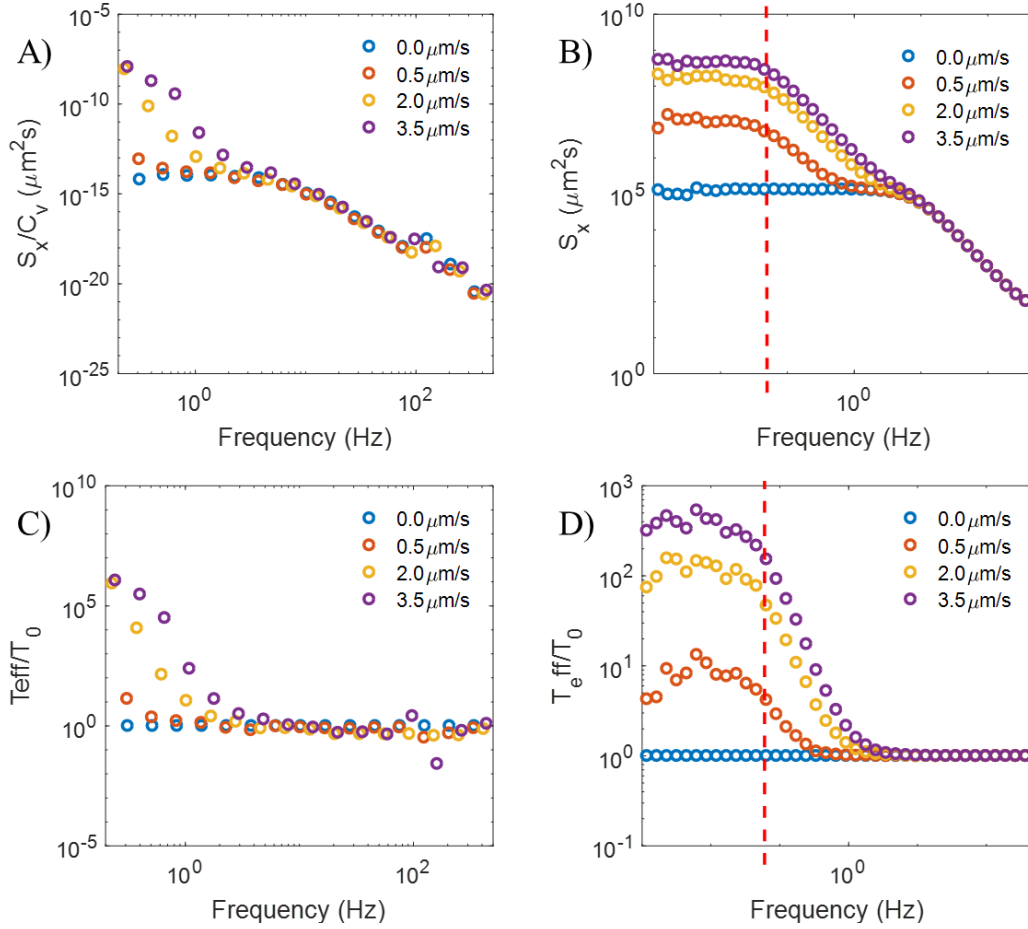


FIG. 5. A) Experimental fluctuation power spectral density (PSD) of 3 μ m Janus particles under 1.5pN/ μ m trap for various AC electric potential at 5 kHz. The black dotted line showing the PSD of a 3 μ m glass particle which overlap with the Janus particle at 0V. B) Simulated fluctuation power spectral density (PSD) of Active particle with rotational diffusivity equal to 0.05/s under parabolic potential with spring constant equal to 1.5pN/ μ m for various particle speed from 0.0 μ m/s to 3.5 μ m/s. The low frequency turning points appear as the redline showing. C) The effective temperature of 3 μ m Janus particles as a function of frequency with various AC electric potential at 5 kHz. D) The effective temperature of Active particle with rotational diffusivity equal to 0.05/s under parabolic potential with spring constant equal to 1.5pN/ μ m for various particle speed from 0.0 μ m/s to 3.5 μ m/s from the simulation.

Since the high-frequency portion of PSD is similar across all applied voltage, ie., particle active speed, it is possible to normalize across all active speed by the Brownian motion PSD, as shown in Fig 6B. The area under the normalized PSD curves reveals the energy dissipation of only active force. [30] Since the difference of PSD only appears at low frequency, the active force does not contribute to the high-frequency dissipation. Based on classical fluctuation-dissipation theorem, an effective temperature for an ABP can be defined as [31]

$$T_{eff} = \frac{TS_{x,active}(\omega)}{S_{x,passive}(\omega)} \quad (16)$$

With the classical definition, it would appear that the effective temperature has a higher value at low frequency and decrease to ambient temperature at high frequency. As a state

function, the effective temperature should not have a dependence on frequency. This inconsistency on the requirement of effective temperature shows again that in active system classical thermal dynamics needs to be defined and evaluated case by case. Within certain parameter space, the active system may be approximated using a modified definition of state functions such as effective temperature.

The relationship between spatial and temporal fluctuation through effective temperature

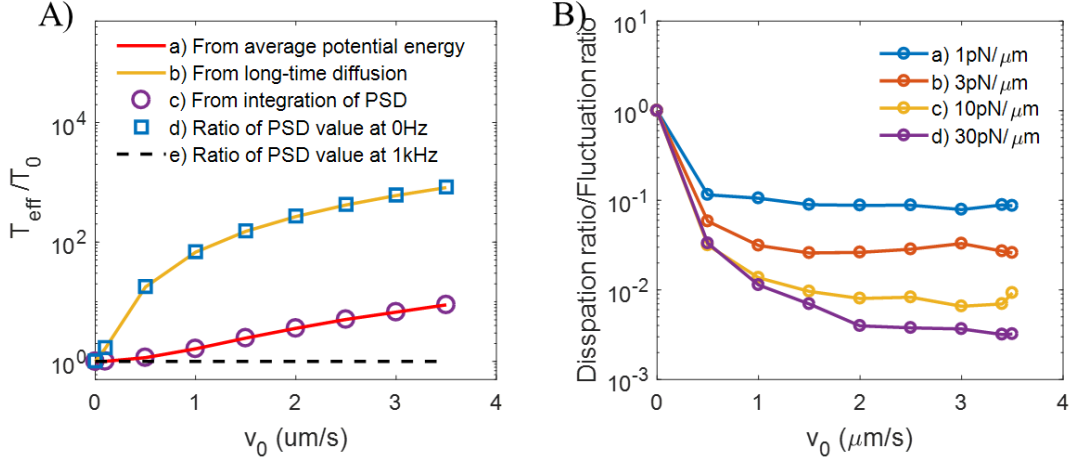


Fig 6. A) Effective temperature from different definitions. B) Energy ratio / Diffusion ratio at different trap stiffness

Although the histogram of an active particle in confinement can be numerically solved by simulation, an analytical solution for it is still missing. We find an analytical solution for the average potential energy of an active particle in a trap, based on the PSD.

In our simulation, it is showing in Fig.6 A, all five effective temperatures from active diffusivity, from potential energy, from fluctuation-dissipation theory (low frequency and high-frequency limit). The zero-frequency ratio from PSD is about equal to the diffusivity ratio. The agreement here can be derived from the previous temporal fluctuation section. The equivalent here comes from the kinematic description of the system. The high-frequency limit ratio from PSD is equal to ambient temperature. The effective temperature from average PSD shows that it deviated from diffusion, but it overlaps with effective temperatures from average potential energy. It seems to be a surprise at the first glance, the reason of this to happen is because of the math. The integration of PSD gives

$$\begin{aligned}
 & \int_0^\infty S_{xx} d\omega \\
 &= \int_0^\infty \frac{1}{T} \int_0^T \int_0^T \langle x(t)x(t') \rangle e^{i\omega(t-t')} dt dt' d\omega \\
 &= \frac{1}{T} \int_0^T \int_0^T \langle x(t)x(t') \rangle \delta(t-t') dt dt' = \frac{1}{T} \int_0^T \langle x^2 \rangle dt
 \end{aligned} \tag{17}$$

Which is equal to average potential energy over trap stiffness. The average energy from spatial fluctuation and temporal fluctuation give the same average energy.

By calculating the ratio of energy ratio over diffusion ratio, which refer to the average potential energy over average long-time diffusivity, we observe that the ratio value decreases and reach platform with increasing the particle speed. For passive particles, this ratio should always be 1. The smaller number refers to less energy dissipation compare with a hot Brownian particle. We also find that the ratio decreases with increasing the trap stiffness. The ratio here is dependent on trap stiffness, which suggesst only part of the dissipation is counting here. The PSD only reveal the dissipation through the particle body but not the flow around it. Also, the trap stiffness dependent also echo that the wall interaction could slowdown the single active particle. [32]

Conclusions

Our study addresses the question of when and how the Boltzmann statistics failed by study the spatial and temporal fluctuation of an active particle in quadratic confinement. Specifically, we measured the fluctuation power spectra and the histograms of individual ICEP-driven metallic Janus particles in an optical trap and compared them to that of non-driven metallic Janus particle.

The experiments and simulations of spatial fluctuation (histogram) of an active particle reveal a new regime of the histogram where the thermal fluctuation dominate the spatial distribution. By using a convolution method, the thermal and non-thermal fluctuation could be decoupled. The histogram of active fluctuation or thermal fluctuation with the larger mean squared displacement determine mostly the total histogram

The experiments and simulations of temporal fluctuation (PSD) of an active particle. The PSD of lower frequency limit yields the effective temperature while the high frequency gives the ambient temperature. We also observed two characteristic time scales in the PSD of the active Brownian particles in a potential well. The extra characteristic time signifies the particles' rotational diffusion coefficient.

By calculating the effective temperature, we found the kinetic expression and energy expression give different value. The effective temperature from energy is dependent on the spring constant. The mean squared displacement from the histogram is equation to the integral of PSD of the active particle at the same condition.

Unlike living cell, we have a well-defined potential filed with a known active particle. Thus, we distinguished the fluctuation is purely from the particle and demonstrate the breakdown of fluctuation-dissipation relation. Since active matter plays a central role in many systems, including, our findings show limitations to apply thermodynamic relations in their classical formulation to study systems with active, non-thermal noise.

ACKNOWLEDGEMENTS

The authors thank Dr. James Gilchrist, Mis. Thitiporn Orm Aewpetch, and Mr. William Mushock for their generous help of preparing the Janus particles. The work was supported in part by the Lehigh Physics Department, the Emulsion Polymers Institute.

References

- [1] A. Sommerfeld, *Thermodynamics and Statistical Mechanics* (1956).
- [2] M. C. Marchetti, J. F. Joanny, S. Ramaswamy, T. B. Liverpool, J. Prost, M. Rao, and R. A. Simha, *Rev. Mod. Phys.* (2013).
- [3] S. Ramaswamy, *Annu. Rev. Condens. Matter Phys.* (2010).
- [4] É. Fodor, C. Nardini, M. E. Cates, J. Tailleur, P. Visco, and F. Van Wijland, *Phys. Rev. Lett.* (2016).
- [5] S. C. Takatori and J. F. Brady, *Phys. Rev. E - Stat. Nonlinear, Soft Matter Phys.* (2015).
- [6] U. Basu, S. N. Majumdar, A. Rosso, and G. Schehr, *Phys. Rev. E* (2018).
- [7] D. Loi, S. Mossa, and L. F. Cugliandolo, *Phys. Rev. E - Stat. Nonlinear, Soft Matter Phys.* (2008).
- [8] J. Palacci, C. Cottin-Bizonne, C. Ybert, and L. Bocquet, *Phys. Rev. Lett.* (2010).
- [9] W. Uspal, M. Popescu, S. Dietrich, M. T.-S. Matter, and undefined 2015, *Pubs.Rsc.Org* (n.d.).
- [10] C. Bechinger, R. Di Leonardo, H. Löwen, C. Reichhardt, G. Volpe, and G. Volpe, *Rev. Mod. Phys.* (2016).
- [11] D. Ray, C. Reichhardt, and C. J. O. Reichhardt, *Phys. Rev. E - Stat. Nonlinear, Soft Matter Phys.* (2014).
- [12] D. Frydel and R. Podgornik, *Phys. Rev. E* (2018).
- [13] S. C. Takatori, R. De Dier, J. Vermant, and J. F. Brady, *Nat. Commun.* (2016).
- [14] A. Argun, A. R. Moradi, E. Pinçe, G. B. Bagci, A. Imparato, and G. Volpe, *Phys. Rev. E* (2016).
- [15] H. D. Ou-Yang and C. Shen, in (2018).
- [16] S. Jiang, Q. Chen, M. Tripathy, E. Luijten, K. S. Schweizer, and S. Granick, *Adv. Mater.* (2010).
- [17] T. Muangnapoh, A. L. Weldon, and J. F. Gilchrist, *Appl. Phys. Lett.* (2013).
- [18] S. Gangwal, O. J. Cayre, M. Z. Bazant, and O. D. Velev, *Phys. Rev. Lett.* (2008).
- [19] I. F. Sbalzarini and P. Koumoutsakos, *J. Struct. Biol.* (2005).
- [20] M. T. Valentine, L. E. Dewalt, and H. D. Ou-Yang, *J. Phys. Condens. Matter* (1996).
- [21] M.-T. Wei, A. Zaorski, H. C. Yalcin, J. Wang, M. Hallow, S. N. Ghadiali, A. Chiou, and H. D. Ou-Yang, *Opt. Express* (2008).
- [22] Y. Zong, J. Liu, R. Liu, H. Guo, M. Yang, Z. Li, and K. Chen, *ACS Nano* (2015).
- [23] S. Nedev, S. Carretero-Palacios, P. Kühler, T. Lohmüller, A. S. Urban, L. J. E. Anderson, and J. Feldmann, *ACS Photonics* (2015).
- [24] G. R. Yi, D. J. Pine, and S. Sacanna, *J. Phys. Condens. Matter* (2013).
- [25] G. Volpe, S. Gigan, and G. Volpe, *Am. J. Phys.* (2014).

- [26] T. M. Squires and M. Z. Bazant, J. Fluid Mech. (2006).
- [27] M. C. Marchetti, Y. Fily, S. Henkes, A. Patch, and D. Yllanes, Curr. Opin. Colloid Interface Sci. (2016).
- [28] Fodor, W. W. Ahmed, M. Almonacid, M. Bussonnier, N. S. Gov, M. H. Verlhac, T. Betz, P. Visco, and F. Van Wijland, EPL **116**, (2016).
- [29] R. Kubo, Reports Prog. Phys. (1966).
- [30] E. Ben-Isaac, E. Fodor, P. Visco, F. Van Wijland, and N. S. Gov, Phys. Rev. E - Stat. Nonlinear, Soft Matter Phys. (2015).
- [31] Fodor, M. Guo, N. S. Gov, P. Visco, D. A. Weitz, and F. Van Wijland, EPL (2015).
- [32] A. P. Solon, Y. Fily, A. Baskaran, M. E. Cates, Y. Kafri, M. Kardar, and J. Tailleur, Nat. Phys. **11**, 673 (2015).